© 2014. Published by The Company of Biologists Ltd | Development (2014) 141, 296-306 doi:10.1242/dev.099747

RESEARCH ARTICLE

STEM CELLS AND REGENERATION

Fgf10-positive cells represent a progenitor cell population during lung development and postnatally

Elie El Agha[1,2], Susanne Herold[1,2], Denise Al Alam[3], Jennifer Quantius[2], BreAnne MacKenzie[1,2], Gianni Carraro[1,2], Alena Moiseenko[1,2], Cho-Ming Chao[1,2], Parviz Minoo[4], Werner Seeger[1,2] and Saverio Bellusci[1,2,3,*]

ABSTRACT

The lung mesenchyme consists of a widely heterogeneous population of cells that play crucial roles during development and homeostasis after birth. These cells belong to myogenic, adipogenic, chondrogenic, neuronal and other lineages. Yet, no clear hierarchy for these lineages has been established. We have previously generated a novel *Fgf10*^{iCre} knock-in mouse line that allows lineage tracing of *Fgf10*-positive cells during development and postnatally. Using these mice, we hereby demonstrate the presence of two waves of *Fgf10* expression during embryonic lung development: the first wave, comprising *Fgf10*-positive cells residing in the submesothelial mesenchyme at early pseudoglandular stage (as well as their descendants); and the second wave, comprising *Fgf10*-positive cells from late pseudoglandular stage (as well as their descendants). Our lineage-tracing data reveal that the first wave contributes to the formation of parabronchial and vascular smooth muscle cells as well as lipofibroblasts at later developmental stages, whereas the second wave does not give rise to smooth muscle cells but to lipofibroblasts as well as an Nkx2.1^{-} E-Cad^{-} Epcam^{+} Pro-Spc^{+} lineage that requires further in-depth analysis. During alveologenesis, *Fgf10*-positive cells give rise to lipofibroblasts rather than alveolar myofibroblasts, and during adult life, a subpopulation of *Fgf10*-expressing cells represents a pool of resident mesenchymal stromal (stem) cells (MSCs) (Cd45^{-} Cd31^{-} Sca-1^{+}). Taken together, we show for the first time that *Fgf10*-expressing cells represent a pool of mesenchymal progenitors in the embryonic and postnatal lung. Our findings suggest that *Fgf10*-positive cells could be useful for developing stem cell-based therapies for treating interstitial lung diseases.

KEY WORDS: Lung mesenchyme, Lineage tracing, *Fgf10*-positive cells, Resident MSCs, Mouse

INTRODUCTION

The adult mouse lung consists of at least 40-60 different types of cells that are organized in a highly sophisticated 3D structure inside the thoracic cavity (Crapo et al., 1982; McQualter and Bertoncello, 2012). These cell types can be broadly classified into epithelial cells (populating the airways) and mesenchymal cells (populating the surrounding extracellular matrix). Along the proximodistal axis, the mouse lung is rich with stem/progenitor cells that are capable of self-renewal, multipotent differentiation and pollutant resistance.

Whereas the lineage tree of the lung epithelium has been thoroughly studied during embryonic development and postnatally (Giangreco et al., 2002; Hong et al., 2004; Kim et al., 2005; Rawlins et al., 2009; Rock et al., 2009; Stripp et al., 1995), the lineage tree of the postnatal lung mesenchyme is poorly understood. This part of the lung consists of a wide array of cell types such as smooth muscle cells, endothelial cells, chondrocytes, nerve cells, lipofibroblasts, myofibroblasts, lymphatic cells and others.

Most of our knowledge regarding the lineage tree of the lung mesenchyme has been achieved by studying embryonic development. For example, our research group has previously used a fibroblast growth factor 10 (*Fgf10*)-*lacZ* transgenic line (originally reported as *Mlcv1v-nLacZ-24*) to demonstrate that *Fgf10*-expressing cells are progenitors for parabronchial smooth muscle cells (PBSMCs) in the distal lung during early embryonic development (Mailleux et al., 2005). Shan et al., on the other hand, identified a population of mesenchymal cells, initially located near the lung hilum, as progenitors for airway smooth muscle cells (Shan et al., 2008). Using Wilms tumor 1 homolog (*Wt1*)-*Cre* transgenic line, Que et al. have suggested that the mesothelium is a source of vascular – but not airway – smooth muscle cells (Que et al., 2008). On the contrary, Greif et al. have shown that vascular smooth muscle cells (VSMCs) arise from *Pdgfrb*-positive mesenchymal cells rather than *Wt1*-positive mesothelial cells (Greif et al., 2012). More recently, Dixit et al. utilized *Wt1*$^{Cre\text{-}ERT2/+}$ mice to demonstrate that *Wt1*-positive cells are indeed progenitors for airway and VSMCs as well as desmin^{+} fibroblasts (Dixit et al., 2013). Fetal liver kinase 1 (*Flk-1*; *Kdr* – Mouse Genome Informatics), another term for vascular endothelial growth factor receptor 2 (*Vegfr2*), has been identified as the earliest marker for endothelial progenitors (angioblasts) that respond to Vegfa and give rise to the capillary plexus surrounding the airways (Del Moral et al., 2006; Kappel et al., 1999; Yamaguchi et al., 1993). Using a prospero homeobox 1 (*Prox1*)$^{Cre\text{-}ERT2}$ knock-in line, Srinivasan et al. have shown that lympthatic cells arise from *Prox1*-positive progenitor cells (Srinivasan et al., 2007). Finally, Langsdorf et al. used receptor tyrosine kinase (*Ret*)^{EGFP} knock-in line to transiently trace neuronal progenitors during embryonic development and show that nerve cells originate from the neural crest (Langsdorf et al., 2011).

One of the early markers of the lung mesenchyme is *Fgf10*. During early lung development, *Fgf10* is expressed in the distal (submesothelial) mesenchyme and it acts on the opposite epithelium expressing *Fgfr2b* to maintain the epithelial cells in a progenitor-like state and induce branching and migration (Bellusci et al., 1997; Lü et al., 2005; Park et al., 1998). Gain of function of *Fgf10* during

[1]Excellence Cluster Cardio-Pulmonary System (ECCPS), D-35392 Giessen, Hessen, Germany. [2]Member of the German Center for Lung Research, Department of Internal Medicine II, Universities of Giessen and Marburg Lung Center (UGMLC), D-35390 Giessen, Hessen, Germany. [3]Developmental Biology and Regenerative Medicine Program, Saban Research Institute of Childrens Hospital Los Angeles and University of Southern California, Los Angeles, CA 90027, USA. [4]Department of Pediatrics, Division of Newborn Medicine, University of Southern California, Childrens Hospital Los Angeles, Los Angeles, CA 90027, USA.

*Author for correspondence (saverio.bellusci@innere.med.uni-giessen.de)

Received 3 June 2013; Accepted 15 October 2013

Development (2014) doi:10.1242/dev.099747

development leads to epithelial progenitor state arrest and distalization of the lung (Nyeng et al., 2008; Volckaert et al., 2013), whereas loss of function of *Fgf10* results in branching simplification and decreased numbers of epithelial progenitors. Although the primary target of Fgf10 is the epithelium, severe mesenchymal abnormalities are also observed when Fgf10 signaling is attenuated (Ramasamy et al., 2007).

We have previously generated a novel *Fgf10*$^{Cre\text{-}ERT2/+}$ (or *Fgf10*$^{iCre/+}$) knock-in mouse line that allows specific labeling of *Fgf10*-expressing cells, which can be lineage-traced temporally and spatially (El Agha et al., 2012). Using this line, combined with *tomato*^{flox} Cre-reporter line, we performed extensive lineage tracing of *Fgf10*-positive cells during lung development and postnatal homeostasis. We used a combination of time-lapse imaging, immunofluorescence, fluorescence-activated cell sorting (FACS) analysis and sorting, analysis of cytospin-prepared cells and reverse transcription polymerase chain reaction (RT-PCR) on isolated cells to characterize the progeny of *Fgf10*-expressing cells labeled at distinct time points throughout lung development and postnatally. Our data indicate that *Fgf10*-positive cells represent a pool of progenitors for multiple lineages in the embryonic and postnatal lung mesenchyme.

RESULTS

Fgf10^{iCre} knock-in line is not leaky and does not show signs of ectopic expression

We have previously shown that the *Fgf10*$^{iCre/+}$*; tomato*$^{flox/+}$ lineage-tracing tool allows permanent labeling of *Fgf10*-positive cells (as well as their descendants) and thus opening the way to study their fate in a time-controlled manner (El Agha et al., 2012). To further validate this line, *Fgf10*$^{iCre/+}$*; tomato*$^{flox/flox}$ mice were crossed with the previously established *Fgf10-lacZ* reporter line (Kelly et al., 2001; Mailleux et al., 2005) and pregnant mice received a single intraperitoneal (IP) injection of tamoxifen at embryonic day (E) 11.5 and embryonic lungs were harvested at E13.5 (supplementary material Fig. S1). We reasoned that lineage-labeled cells from E11.5 are likely to retain *Fgf10* expression at E13.5. Double immunostaining for red fluorescent protein (RFP; reporting for *Fgf10*-expressing cells at E11.5 as well as their descendants) and *lacZ* (reporting for total *Fgf10*-expressing cells at E13.5) showed that all lineage-labeled cells were indeed *lacZ* positive, indicating the absence of ectopic expression from the *Fgf10*^{iCre} locus and demonstrating that *Fgf10*-expressing cells are specifically targeted with this tool. Quantification revealed that 65.44±4.27% (n=3) of total *lacZ*-positive cells were also positive for the lineage label (RFP), indicating that this model allows the targeting of a subset of *Fgf10*-expressing cells. Like any other lineage-tracing tool, the level of recombination greatly depends on the dose of tamoxifen used. For this study, a tolerable dose of 0.1 mg/g of body weight was used.

Throughout the study, *Fgf10*$^{+/+}$*; tomato*$^{flox/+}$ littermates from tamoxifen-injected mice and/or *Fgf10*$^{iCre/+}$*; tomato*$^{flox/+}$ offspring from corn-oil-injected mice were used as controls and no recombination was observed in these offspring at the level of whole-mount fluorescence imaging, fluorescence microscopy of lung sections and FACS analysis, confirming the absence of leakiness in the *Fgf10*$^{iCre/+}$*; tomato*$^{flox/+}$ tool.

Fgf10-positive cells are amplified and migrate during early lung development *ex vivo*

In order to study the behavior of *Fgf10*-positive cells during the pseudoglandular stage of lung development, pregnant mice carrying *Fgf10*$^{iCre/+}$*; tomato*$^{flox/+}$ embryos received a single IP injection of tamoxifen at E11.5 and embryos were harvested at E12.5. Lungs were cultured in an air-liquid interphase and brightfield/fluorescence time-lapse imaging was carried out for 72 hours (Fig. 1; supplementary material Movie 1; n=3). Lineage-labeled cells were originally detected as small populations in the distal mesenchyme and were mostly abundant in the accessory lobe (Fig. 1B-B″). During the first 24 hours of culture, tomato-positive cells amplified exponentially and populated other regions of the growing lung (Fig. 1D-D″,J). At the end of the three-day culture, lineage-labeled cells were highly abundant and dispersed throughout the lung mesenchyme (Fig. 1E-E″). After *ex vivo* culture, lungs were fixed, processed and stained for αSma (Acta2 – Mouse Genome Informatics) (Fig. 1F-I). An average of 81±0.2 (n=3) tomato-positive cells was detected per section (Fig. 1G,G′,K) and a subpopulation of *Fgf10*-positive cells (5.67±0.57 cells; n=3) appeared in the PBSMC layer (Fig. 1I,I′,K).

Fgf10-positive cells are progenitors for parabronchial and VSMCs *in vivo*

To study the commitment of *Fgf10*-positive cells to the smooth muscle lineage *in vivo*, pregnant mice carrying *Fgf10*$^{iCre/+}$*; tomato*$^{flox/+}$ embryos received a single IP injection of tamoxifen at E10.5 and embryonic lungs were harvested at E13.5, E15.5 and E18.5 (Fig. 2A-C). Because tomato-positive cells were mostly abundant in the accessory lobe, this lobe was used for immunostaining. αSma staining of *Fgf10*$^{iCre/+}$*; tomato*$^{flox/+}$ lungs revealed a subpopulation of tomato-positive cells in the PBSMC layer at all three developmental stages (Fig. 2G,G′,K,K′,O,O′). Among total tomato-positive cells, tomato-positive PBSMCs were significantly abundant at E13.5 (14.03±1.31% of total tomato-positive cells; n=3) (Fig. 2A) and E15.5 (18.47±3.75%; n=3) (Fig. 2B) but to a less extent at E18.5 (7.51±0.72%; n=3) (Fig. 2C). Another population of tomato-positive cells was identified in the VSMC compartment at E15.5 (3.44±0.96%; n=3) (Fig. 2B; supplementary material Fig. S2) and E18.5 (4.88±0.83%; n=3) (Fig. 2C; supplementary material Fig. S2). A third population of lineage-labeled cells was observed in the vicinity of parabronchial and VSMCs at all three stages. Initially, we thought that these cells could have a neuronal nature, as *Fgf10* is known to be involved in neurogenesis (Haan et al., 2013; Hajihosseini et al., 2008). However, β-III Tubulin (tubulin, beta 3 class III – Mouse Genome Informatics) immunostaining did not show any overlap with the lineage label (data not shown).

Fgf10-positive cells from early pseudoglandular stage are progenitors for smooth muscle cells and lipofibroblasts *in vivo*

The genetic model used in this study revealed that only a minor proportion of *Fgf10*-positive cells commits to the smooth muscle lineage (Fig. 2). *Fgf10* is known to be expressed by adipocyte precursors and *Fgf10*-null neonates suffer from impaired development of the white adipose tissue (Sakaue et al., 2002; Yamasaki et al., 1999). Thus, we decided to investigate whether *Fgf10*-positive cells give rise to an adipose-related cell lineage in the lung, the lipofibroblasts. *Fgf10*-positive cells were labeled during early pseudoglandular stage (E11.5) and lungs were harvested at E12.5, E15.5 and E18.5 (Fig. 3A-C). FACS analysis showed a drastic increase in the total number of RFP^{+} cells from E12.5 to E15.5 and then E18.5 (Fig. 3D). Our unpublished data show that lipofibroblasts start to emerge in the lung at E15.5; thus, αSma and Adrp (Plin2 – Mouse Genome Informatics) immunostaining was performed at E18.5. For convenience, the left lung lobe was used to carry out immunofluorescence staining and quantification (Fig. 3F). An average of 450±10.12 (n=3) tomato-positive cells was counted per sample and a minor proportion of RFP-positive cells stained for

Development (2014) doi:10.1242/dev.099747

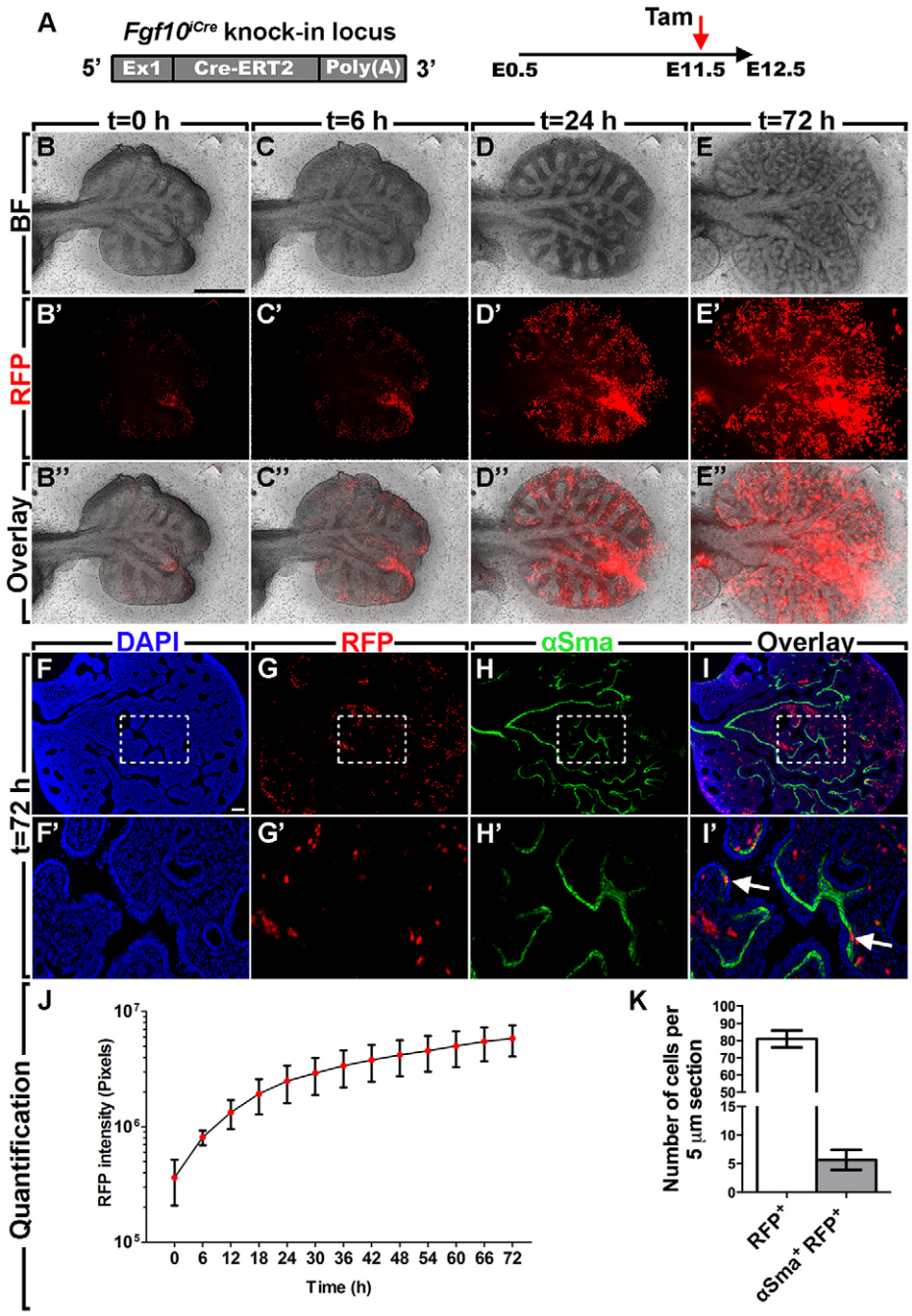

Fig. 1. Time-lapse imaging of E12.5 lungs from *Fgf10*$^{iCre/+}$; *tomato*$^{flox/+}$ embryos.
(A) Schematic of the *Fgf10* locus in *Fgf10*^{iCre} knock-in mice. Recombination was induced *in vivo* by a single IP injection of tamoxifen at E11.5. (B-E) Brightfield imaging of an E12.5 *Fgf10*$^{iCre/+}$; *tomato*$^{flox/+}$ lung undergoing branching morphogenesis. (B′-E′) Whole-mount fluorescence imaging showing the progressive amplification and migration of lineage-labeled cells. Note the high tomato expression in the accessory lobe at t=0 hour. (B″-E″) Overlay of brightfield and fluorescent images.
(F-I) Immunofluorescent detection of αSma (green) in the lung after 72 hours of culture. The areas in white boxes are magnified in F′-I′. A subpopulation of lineage-labeled cells lies in the PBSMC layer (white arrows in I′).
(J) Quantification of the RFP signal over time.
(K) Quantification of lineage-labeled cells after αSma immunostaining. *n*=3. Data are shown as average values ± s.e.m. Scale bars: 500 μm (B-E); 75 μm (F-I). BF, brightfield.

αSma around the epithelium (5.68±0.39%; *n*=3) (Fig. 3E,G) and within vascular walls (4.31±0.23%; *n*=3) (Fig. 3E,H). Similarly to *Fgf10*-positive cells labeled at E10.5, a population of αSma^{-} RFP^{+} cells was identified in the vicinity of PBSMCs (10.17±0.88%; *n*=3) (Fig. 3E,I) and VSMCs (3.92±0.72%; *n*=3) (Fig. 3E). These cells did not express the neuronal marker *β-III tubulin* (supplementary material Fig. S3). However, a significant population of RFP-positive cells stained for Adrp (29.96±5.17%; *n*=3) (Fig. 3E,J) and the remaining population of RFP-positive cells (45.97±4.2%; *n*=3) that did not stain for αSma or Adrp was characterized by its big size and the presence of filopodia (Fig. 3E,K). The lungs were also stained for other markers, such as Cd45 (Ptprc – Mouse Genome Informatics) and Cd31 (Pecam1 – Mouse Genome Informatics), but no overlap was observed between these markers and the RFP signal (supplementary material Fig. S3).

Fgf10-positive cells from late pseudoglandular stage are progenitors for lipofibroblasts *in vivo*

Fgf10-positive cells from E11.5 showed to be precursor cells for PBSMCs, VSMCs and lipofibroblasts at E18.5 (Fig. 3). However, the commitment of these early progenitors to the smooth muscle lineage showed a decline beyond E15.5 (Fig. 2). To investigate this observation further and to test whether lipofibroblast progenitors are restricted to early developmental stages, *Fgf10*-positive cells were labeled at E15.5 and embryonic lungs were harvested at E16.5 and E18.5 (Fig. 4). RFP expression was low at E16.5 (Fig. 4A) and was more pronounced at E18.5 (Fig. 4B). The left lung lobe was used to carry out immunofluorescence staining and quantification (Fig. 4D). An average of 499±71.04 (*n*=3) tomato-positive cells was counted per sample at E18.5 and αSma staining showed minimal overlap with the RFP signal in the parabronchial (0.26±0.03%; *n*=3) and

Development (2014) doi:10.1242/dev.099747

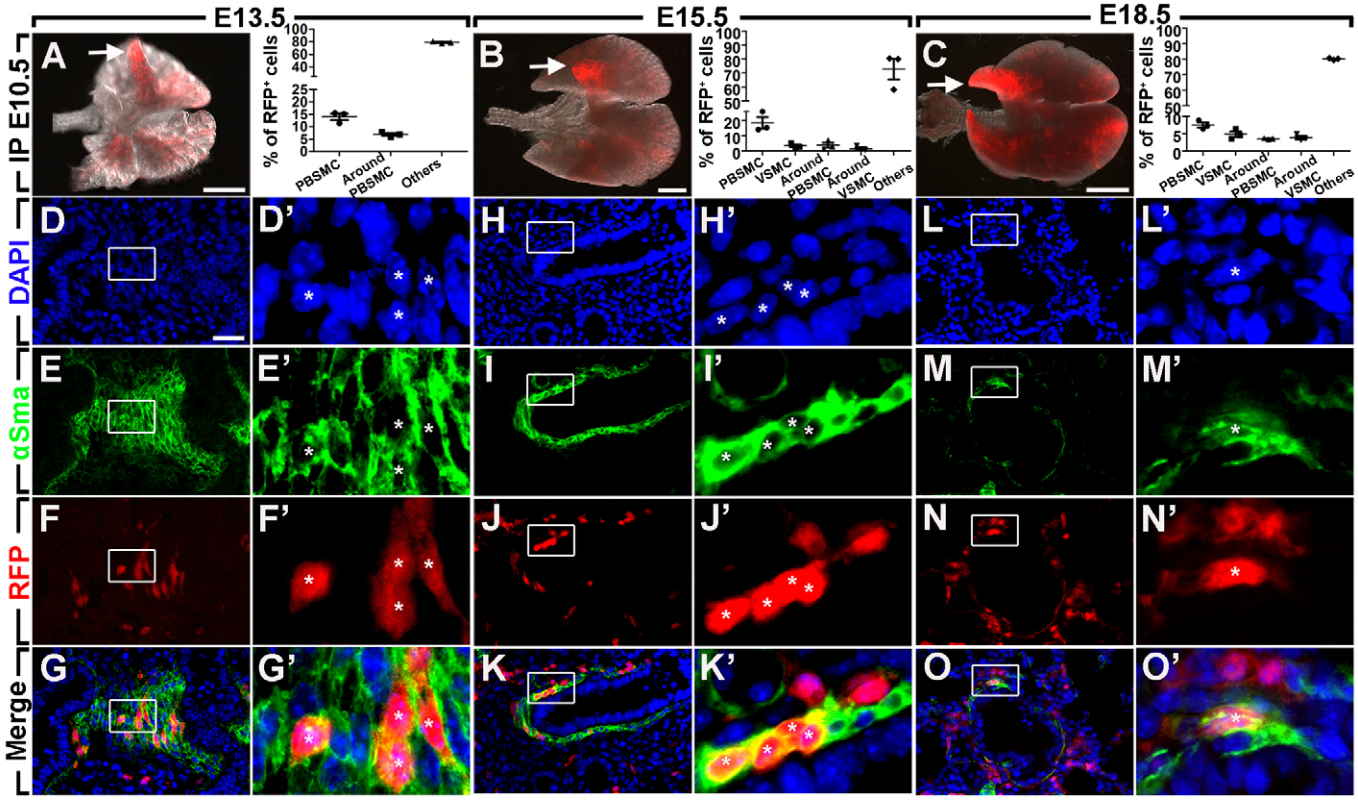

Fig. 2. Contribution of *Fgf10*-positive cells labeled at E10.5 to the parabronchial smooth muscle lineage *in vivo*. (A-C) Overlay of brightfield and whole-mount fluorescent images of the lung at E13.5, E15.5 and E18.5. Note the strong RFP signal in the accessory lobe at all three stages (white arrows). The right panels in A-C show the quantification of multiple RFP$^+$ populations based on αSma staining for each stage. (D-O) Single-channel and merged images of αSma staining (green) of the accessory lobes of the lungs from the upper panel showing RFP-positive cells (red) in the PBSMC layer at all three stages (asterisks). The areas in the white boxes are magnified in D′-O′. *n*=3. Data are shown as average values ± s.e.m. Scale bars: 500 µm (A); 1000 µm (B); 750 µm (C); 25 µm (D-O).

vascular (0.75±0.34%; *n*=3) compartments (Fig. 4E). Significant numbers of αSma$^-$ RFP$^+$ cells around PBSMCs (10.33±1.65%; *n*=3) (Fig. 4E,F) and VSMCs (4.99±0.32%; *n*=3) (Fig. 4E,G) were detected and Adrp staining revealed a considerable proportion of Adrp$^+$ RFP$^+$ cells (39.98±8.28%; *n*=3) (Fig. 4E,H,I). Similarly to cells labeled at E11.5, αSma$^-$Adrp$^-$ β-III Tub$^-$ Cd45$^-$ Cd31$^-$ cells (43.69±8.32%; *n*=3) were also observed (Fig. 4E,J,K; supplementary material Fig. S3).

Fgf10 expression identifies lipofibroblast rather than alveolar myofibroblast progenitors during alveologenesis

The alveolar stage of lung development is known for the prevalence of alveolar myofibroblasts. These cells, in addition to lipofibroblasts, are believed to play a crucial role in secondary septa formation and alveolar maturation during postnatal alveolarization (O'Hare and Sheridan, 1970; Rehan and Torday, 2012; Rubin et al., 2004; Torday and Rehan, 2007; Vaccaro and Brody, 1978; Yamada et al., 2005). To determine whether *Fgf10*-positive cells contribute to these lineages postnatally, pregnant mice carrying *Fgf10$^{iCre/+}$; tomato$^{flox/+}$* embryos were left to develop to term and then fed tamoxifen-containing pellets starting on postnatal day 2 (P2). At P14, pups were sacrificed, lungs were harvested, and the left lung lobe was used for immunostaining (Fig. 5). No tomato signal was detected in lungs from *Fgf10$^{+/+}$; tomato$^{flox/+}$* pups (Fig. 5A,L) whereas the signal was abundant in their *Fgf10$^{iCre/+}$; tomato$^{flox/+}$* counterparts (Fig. 5B), especially near the main bronchus (Fig. 5C). An average of 141±40 (*n*=3) tomato-positive cells was counted per *Fgf10$^{iCre/+}$; tomato$^{flox/+}$* sample and αSma immunostaining revealed a subpopulation of lineage-labeled cells expressing *αSma* (19.70±1.88%; *n*=3) (Fig. 5D-H,M). These cells were located in the lung parenchyma and not at the tips of secondary septa. On the other hand, Adrp immunostaining showed that a major proportion of *Fgf10*-expressing cells gives rise to lipofibroblasts (67.74±1.27%; *n*=3) (Fig. 5I-K,M).

Fgf10-positive cells from various developmental stages exhibit various molecular signatures and are retained postnatally

Fgf10-expressing cells were labeled at E11.5 or E15.5 and lungs were harvested at E18.5. Lungs were dissociated into single-cell suspensions and stained for Cd45, Cd31, Epcam, Pdgfra, Kit and Sca-1 (Ly6a – Mouse Genome Informatics). A FACSAria III cell sorter was used to analyze 50,000-100,000 cells per sample per time point. No tomato signal was detected in lungs from *Fgf10$^{+/+}$; tomato$^{flox/+}$* embryos (Fig. 6A) or from *Fgf10$^{iCre/+}$; tomato$^{flox/+}$* embryos exposed to corn oil instead of tamoxifen (data not shown). Whereas lineage-labeled cells from E11.5 accounted for ~0.5% of the total lung, those from E15.5 accounted for ~1.5% (Fig. 6B,C) and most of these cells were Cd45$^-$ Cd31$^-$ (data not shown). Almost all lineage-labeled cells from both time points expressed low levels of *Sca-1* (Sca-1^{low}) at E18.5 (Fig. 6E,G) and a subpopulation of *Fgf10*-positive cells from E11.5 and E15.5 also expressed the

Development (2014) doi:10.1242/dev.099747

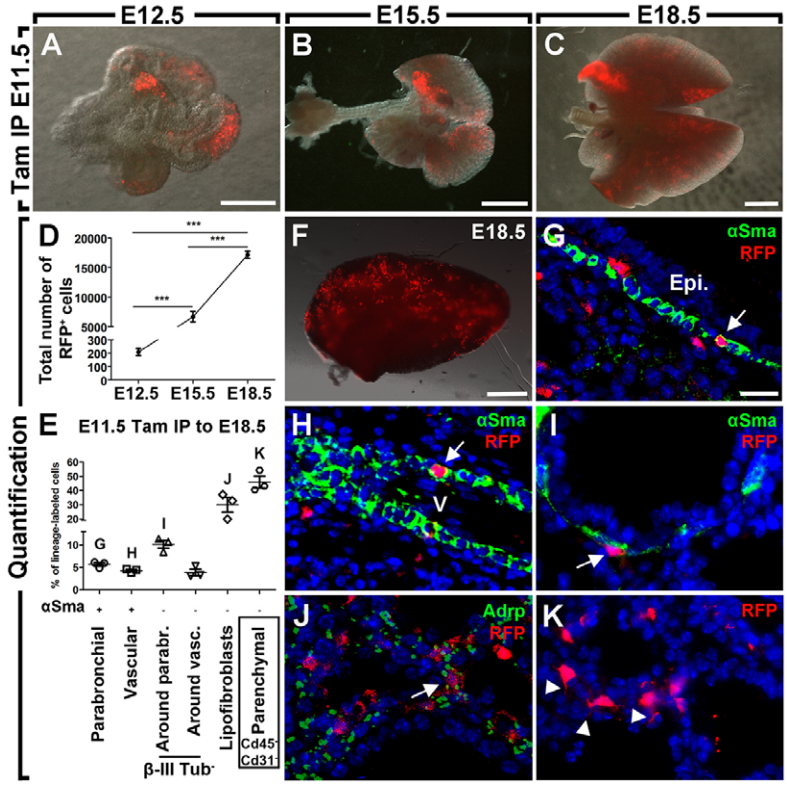

Fig. 3. *In vivo* lineage tracing of *Fgf10*-positive cells labeled at E11.5. (A-C) Overlay of brightfield and whole-mount fluorescent images of the lung at E12.5, E15.5 and E18.5. (D) The total number of RFP$^+$ cells in the lungs shown in A-C increases drastically over time, as determined by FACS analysis. (E) Quantification of RFP-positive populations. (F) Overlay of brightfield and whole-mount fluorescent images of the left lung lobe at E18.5. (G-I) αSma staining showing RFP-positive cells in the PBSMC layer (G), vascular walls (H) and around PBSMCs (I). (J) Immunofluorescence staining showing an Adrp$^+$ RFP$^+$ cell. (K) Big RFP-positive cells with filopodia (arrowheads) are present in the lung parenchyma. *n*=3. Data are shown as average values ± s.e.m. ***P<0.001 (one-way ANOVA). Scale bars: 250 µm (A); 1000 µm (B,C); 500 µm (F); 12.5 µm (G-K). Epi, epithelium; v, vessel.

mesenchymal marker *Pdgfra* at E18.5 (~9.9% and ~17.5%, respectively) (Fig. 6F,H). Interestingly, almost no tomato-positive cells from E11.5 and ~18.1% from E15.5 stained for the pan-epithelial cell marker *Epcam* at E18.5 (Fig. 6E,G). *Kit* expression was very low at this stage (E18.5) but staining revealed ~7.3% and ~1.4% overlap with the tomato signal in E11.5 and E15.5 time points, respectively (Fig. 6F,H). RT-PCR and cytospin analysis of sorted *Fgf10*-positive cells (labeled at E15.5) showed high expression of *Adrp* (Fig. 6D), confirming the immunofluorescence data obtained from processed lung tissues (Figs 3 and 4). Histological analysis of E15.5 *Fgf10*$^{iCre/+}$*; tomato*$^{flox/+}$ lungs (labeled at E11.5) showed a subpopulation of RFP$^+$ Pdgfra$^+$ cells (Fig. 6I,J).

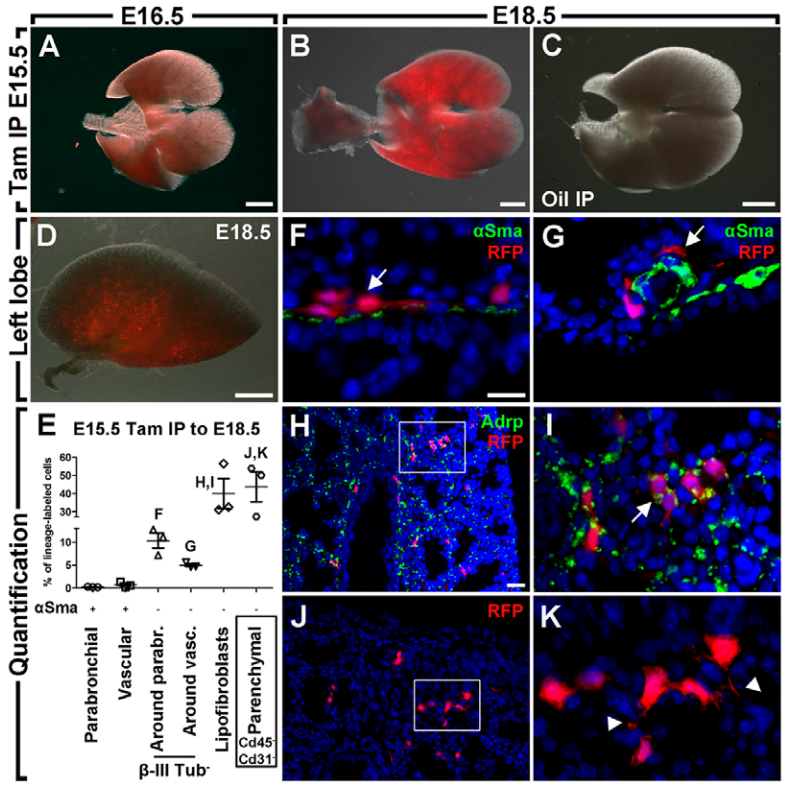

Fig. 4. *In vivo* lineage tracing of *Fgf10*-positive cells labeled at E15.5. (A,B) Overlay of brightfield and whole-mount fluorescent images of the lung at E16.5 and E18.5. The RFP signal is more intense at E18.5 than at E16.5. (C) Overlay of brightfield and whole-mount fluorescent images of an E18.5 *Fgf10*$^{iCre/+}$*; tomato*$^{flox/+}$ lung exposed to corn oil instead of tamoxifen. (D) Overlay of brightfield and whole-mount fluorescent images of the left lung lobe at E18.5. (E) Quantification of RFP-positive populations. (F,G) αSma staining showing αSma$^-$ RFP$^+$ cells around PBSMCs and VSMCs. (H,I) Adrp immunostaining showing Adrp$^+$ RFP$^+$ cells. The area in the white box is magnified in I. (J,K) Big RFP-positive cells with filopodia (arrowheads) are present in the lung parenchyma. The area in the white box is magnified in K. *n*=3. Data are shown as average values ± s.e.m. Scale bars: 750 µm (A,D); 1000 µm (B,C); 12.5 µm (F,G,I,K); 25 µm (H,J).

Development (2014) doi:10.1242/dev.099747

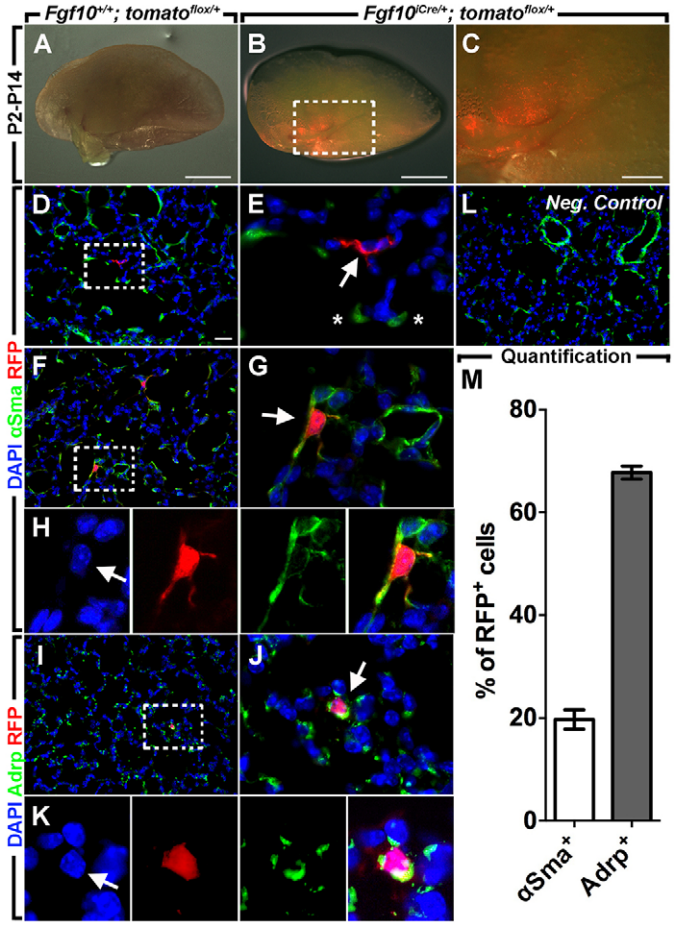

Fig. 5. *Fgf10*-positive cells preferentially give rise to lipofibroblasts rather than alveolar myofibroblasts during alveologenesis. Nursing female mice were fed tamoxifen-containing pellets from P2 to P14. (A) Overlay of brightfield and whole-mount fluorescent images of the left lung lobe from an *Fgf10*$^{+/+}$; *tomato*$^{flox/+}$ pup. (B,C) Representative image of the left lung lobe from *Fgf10*$^{iCre/+}$; *tomato*$^{flox/+}$ pups. Note the strong tomato signal around the mainstem bronchus (C; higher magnification of the boxed area in B). (D,E) Immunostaining for αSma showing an αSma^{-} RFP^{+} cell. The area in the dashed box is magnified in E. The asterisks mark alveolar myofibroblasts in the secondary septa. (F,G) Immunostaining for αSma showing an αSma^{+} RFP^{+} cell (white arrow). The area in the dashed box is magnified in G. (H) Single-channel fluorescent images of the αSma^{+} RFP^{+} cell shown in G. (I,J) Immunostaining for Adrp showing an Adrp^{+} RFP^{+} cell. The area in the dashed box is magnified in J. (K) Single-channel fluorescent images of the Adrp^{+} RFP^{+} cell shown in J. (L) Immunostaining for αSma of an *Fgf10*$^{+/+}$; *tomato*$^{flox/+}$ lung. (M) Quantification of lineage-labeled cells according to *αSma* and *Adrp* expression. *n*=3. Data are shown as average values ± s.e.m. Scale bars: 2.5 mm (A,B); 750 µm (C); 25 µm (D-L).

Fgf10-expressing cells, labeled postnatally, represented ~0.1% of the total lung (a total of one million cells was analyzed) (Fig. 6L). ~15.7% and ~22.8% of total RFP-positive cells stained for Epcam and Sca-1, respectively (Fig. 6M). A subpopulation (accounting for ~10.5% of total RFP-positive cells) exhibited the molecular signature of resident MSCs (Cd45^{-} Cd31^{-} Sca-1^{+}) (Fig. 6N).

In a separate experiment, pregnant mice carrying *Fgf10*$^{iCre/+}$; *tomato*$^{flox/+}$ embryos received a single IP injection of tamoxifen or corn oil at E11.5 and were left to develop to term. The pups from these mice were sacrificed at P30 and lungs were harvested for FACS analysis. Lungs from corn-oil-exposed pups revealed no tomato expression (Fig. 6S), whereas lineage-labeled cells from tamoxifen-exposed lungs appeared in the distal mesenchyme, especially at the tip of the accessory lobe (Fig. 6T,U). These cells accounted for ~0.4% of total lung suspensions (Fig. 6O) and similarly to the cells labeled at E11.5 and harvested at E18.5, minimal overlap between tomato and Epcam was detected (Fig. 6P). Nevertheless, ~11.1% of total lineage-labeled cells expressed *Sca-1*, half of which representing a subset of resident MSCs (Fig. 6P,Q). LipidTOX™ staining revealed that most tomato-positive cells (~83.7%) contained neutral lipids at P30 (Fig. 6R).

In order to further characterize Epcam^{+} RFP^{+} cells, *Fgf10*-expressing cells were labeled at E15.5 and RFP^{+} cells were sorted at E18.5 and stained for Pro-Spc (Sftpc – Mouse Genome Informatics) and E-Cadherin (Cdh1 – Mouse Genome Informatics) (Fig. 7A,B). Interestingly, a subpopulation of RFP^{+} cells was Pro-Spc^{+} but E-Cad^{-} (Fig. 7A′,B′). A similar observation was made for lung sections where RFP^{+} cells could not be detected in the lung epithelium (E-Cad^{-}) (Fig. 7D,D′,F) and 20.23±0.89% (*n*=3) of total RFP^{+} cells was Pro-Spc^{+} (Fig. 7C,C′,F). Finally, RT-PCR on sorted cells (labeled at P2 and collected at P30) showed that Epcam^{+} RFP^{+} cells were positive for *Spc*, but negative for *Nkx2.1* and *E-Cad*, whereas Epcam^{+} RFP^{-} cells were positive for *Nkx2.1*, *E-Cad* and *Spc*. Both populations showed lack of *Fgf10* expression (Fig. 7E).

DISCUSSION

The embryonic lung mesenchyme consists of cells that belong to distinct lineages, including myogenic, adipogenic, chondrogenic, neuronal and other lineages. Most of these cell types arise from endogenous (or resident) progenitor populations whereas few (e.g. nerve cells) arise from exogenous sources (the neural crest). Cell-fate determination probably arises from a complex network of autocrine and paracrine signals leading to the proliferation and differentiation of lineage-restricted as well as multipotent progenitor cell populations.

Fgf10 is an early marker for the submesothelial mesenchyme (Bellusci et al., 1997) and its expression levels have shown to be crucial for the maintenance of both epithelial and mesenchymal progenitors (Ramasamy et al., 2007). The domain of *Fgf10* expression in the embryonic lung has been thoroughly studied. Northern blotting and quantitative PCR (qPCR) data show that *Fgf10* transcripts progressively accumulate in the embryonic lung between E11.5 and E18.5 (Bellusci et al., 1997; El Agha et al., 2012). *In situ* hybridization for *Fgf10* and X-Gal staining of *Fgf10-lacZ* lungs show that *Fgf10* expression is restricted to the tips of the distal mesenchyme until E14.5, after which the expression becomes dispersed throughout the mesenchyme (El Agha et al., 2012; Mailleux et al., 2005; Ramasamy et al., 2007; Tiozzo et al., 2012). Our lineage-tracing data reveal two waves of *Fgf10* expression, each of which is characterized by a distinct pattern in terms of cell localization as well as differentiation potential (Fig. 8A). The first wave, consisting of *Fgf10*-positive cells labeled at E11.5 as well as their descendants, yields cells residing mostly in the distal mesenchyme at E18.5 (especially observed in the accessory lobe) and contributes to myogenic (PBSMCs and VSMCs) as well as adipogenic (lipofibroblasts) lineages. By contrast, the second wave, consisting of *Fgf10*-positive cells labeled at E15.5 as well as their descendants, yields cells that are dispersed throughout the mesenchyme at E18.5 and gives rise to adipogenic, but not myogenic, lineages.

Lineage tracing of *Fgf10*-positive cells from E10.5 showed that these cells contribute to the smooth muscle cell lineage when examined at E13.5, E15.5 and E18.5; however, the percentage of

Development (2014) doi:10.1242/dev.099747

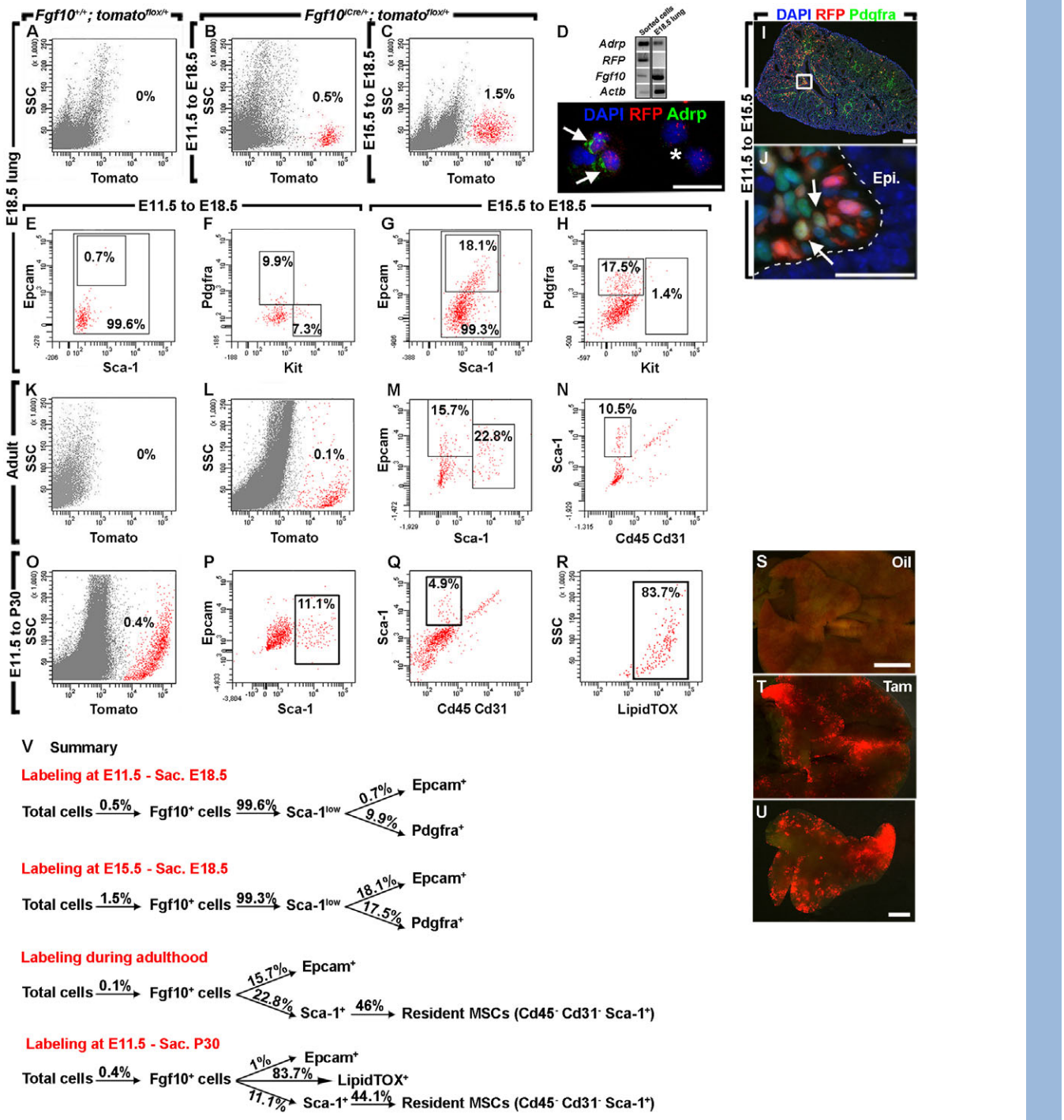

Fig. 6. Flow cytometry analysis of the *Fgf10*-expressing lineage during embryonic development and postnatally. (A) E18.5 lungs from *Fgf10*$^{+/+}$; *tomato*$^{flox/+}$ embryos show no tomato signal. (B,C) Tomato-positive cells account for ~0.5% and ~1.5% of the total E18.5 lung suspension when labeled at E11.5 and E15.5, respectively. (D) RT-PCR and immunostaining of sorted *Fgf10*-positive cells (labeled at E15.5) show high expression of *Adrp* (white arrows). Note the presence of Adrp^{-} cells (asterisk). (E,F) Almost all *Fgf10*-expressing cells labeled at E11.5 express low levels of *Sca-1* (Sca-1^{low}) (E) and ~9.9% of these cells co-express *Pdgfra* (F). (G) Almost all *Fgf10*-expressing cells labeled at E15.5 express low levels of *Sca-1* (Sca-1^{low}) and ~18.1% of these cells co-express *Epcam*. (H) ~17.5% of lineage-labeled cells express *Pdgfra*. (I,J) Section of an E15.5 *Fgf10*$^{iCre/+}$; *tomato*$^{flox/+}$ lung (labeled at E11.5) showing *Pdgfra* expression (green). The area in the white box is magnified in J. White arrows indicate RFP^{+} Pdgfra^{+} cells and the dashed line marks the epithelial-mesenchymal boundary. (K) Lungs from *Fgf10*$^{+/+}$; *tomato*$^{flox/+}$ adult mice show no tomato signal when exposed to tamoxifen. (L) Tomato-positive cells account for ~0.1% of the total adult lung. (M) ~15.7% and ~22.8% of lineage-labeled cells express *Epcam* and *Sca-1*, respectively. (N) A subpopulation of *Fgf10*-expressing cells (~10.5%) shows the molecular signature of resident MSCs. (O) Tomato-positive cells from E11.5 are retained at P30, and account for ~0.4% of the total lung. (P) ~11.1% total RFP^{+} cells express *Sca-1* whereas minimal overlap with *Epcam* expression can be detected. (Q,R) ~4.9% of total tomato-positive cells are resident MSCs (Q) and the majority (~83.7%) of total labeled cells contains neutral lipids (R). (S-U) Whole-mount fluorescence images of lungs from P30 mice that were exposed to corn oil or tamoxifen at E11.5. Note the absence of tomato expression in corn-oil-exposed lungs. The accessory lobe of the tamoxifen-exposed lung shown in T is shown in U. Note the strong tomato signal at the tip of this lobe. (V) Summary of the flow cytometry analysis of the *Fgf10*-expressing lineage during embryonic lung development and postnatally. $n \geq 2$. Scale bars: 25 µm (D); 100 µm (I); 12.5 µm (J); 5 mm (S,T); 2.5 mm (U). Epi, epithelium.

Development (2014) doi:10.1242/dev.099747

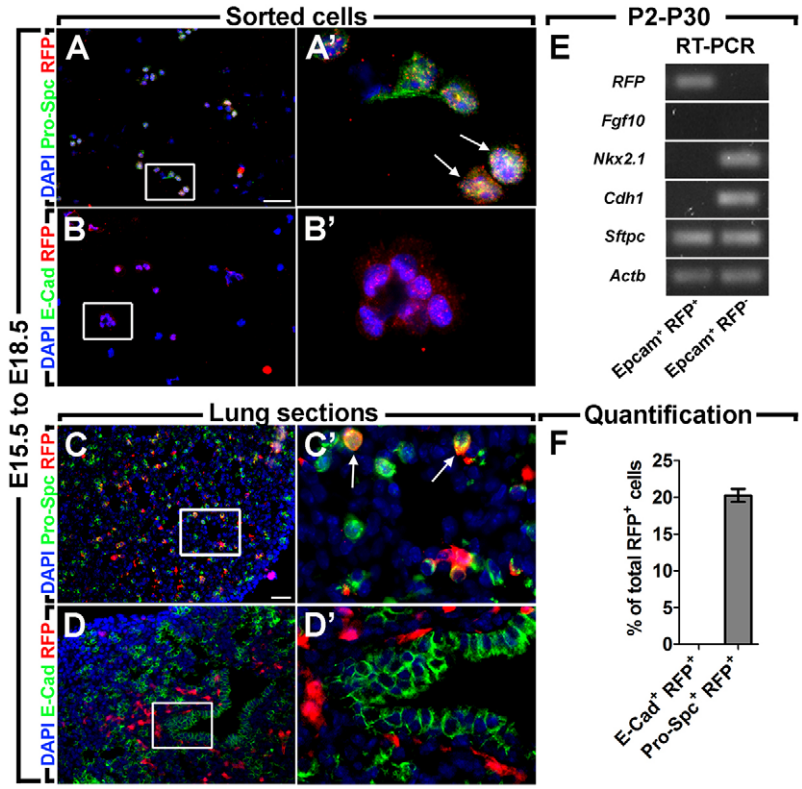

Fig. 7. Epcam$^+$ lineage-labeled cells do not represent an epithelial lineage in the lung. (A-B′) Immunofluorescence staining of sorted *Fgf10*-positive cells (labeled at E15.5 and harvested at E18.5) showing E-Cad$^-$ Pro-Spc$^+$ RFP$^+$ cells. The areas in the white boxes are magnified in A′,B′. The white arrows indicate Pro-Spc$^+$ RFP$^+$ cells. (C,C′) Immunofluorescence staining of lung cryosections (exposed to tamoxifen at E15.5 and harvested at E18.5) showing Pro-Spc$^+$ RFP$^+$ cells in the lung mesenchyme. (D,D′) Immunofluorescence staining of lung sections showing E-Cad$^-$ RFP$^+$ cells. The areas in the white boxes in C,D are magnified in C′,D′. The white arrows indicate Pro-Spc$^+$ RFP$^+$ cells. (E) RT-PCR on sorted cells (labeled at P2 and harvested at P30) showing that Epcam$^+$ RFP$^+$ cells co-express *Spc*, but not *Nkx2.1* or *E-Cad* whereas Epcam$^+$ RFP$^-$ cells co-express *Nkx2.1*, *E-Cad* and *Spc*, but not *Fgf10*. Note the absence of *Fgf10* expression also in Epcam$^+$ RFP$^+$ cells. (F) Quantification of E-Cad$^+$ RFP$^+$ and Pro-Spc$^+$ RFP$^+$ cells from the staining shown in C,D. *n*=3. Scale bars: 50 µm (A,B); 25 µm (C,D).

αSma$^+$ RFP$^+$ cells relative to total RFP$^+$ cells showed a decline between E15.5 and E18.5. As the overall number of *Fgf10*-positive cells (labeled at E11.5) showed a drastic increase from E12.5 to E15.5 and then E18.5 as demonstrated by FACS analysis (also demonstrated by time-lapse imaging of E12.5 lung undergoing branching morphogenesis), we conclude that the drop in the number of αSma$^+$ RFP$^+$ cells relative to total RFP$^+$ cells at E18.5 is likely to be due to the expansion of the αSma$^-$ RFP$^+$ population at the expense of the αSma$^+$ RFP$^+$ population. In other words, the limited αSma$^+$ RFP$^+$ fraction that forms between E10.5 and E15.5 gets diluted in the αSma$^-$ RFP$^+$ population, which continues to expand beyond E15.5. This is supported by our observation that αSma$^+$ cells rarely proliferate when examined at E13.5, E15.5 and E18.5 (supplementary material Fig. S4). The proliferative capacity of *Fgf10*-positive cells was also demonstrated by time-lapse imaging of E18.5 lung explants that were induced with tamoxifen at E11.5 (supplementary material Movie 2) or E15.5 (data not shown). Moreover, primary cultures of E18.5 lung mesenchyme (induced with tamoxifen at E11.5 or E15.5) showed that ~40% of RFP$^+$ cells were undergoing mitosis during the 24 hours of culture (supplementary material Movie 3).

It was recently reported that a multipotent cardiopulmonary progenitor cell population (Wnt2$^+$ Gli1$^+$ Isl1$^+$), originating from the second heart field (SHF), invades the lung, giving rise to airway and VSMCs in addition to other lineages (Peng et al., 2013). Our lineage-tracing system does not label any SHF cells as lineage-labeled cells could not be detected in the heart at any given time point, probably owing to the deletion of intronic sequences containing transcription factor binding sites for Isl1, Nkx2.5, Tbx5 and others (El Agha et al., 2012). Yet the possibility that a subset of *Fgf10*-positive cells arises from *Isl1*-positive cells coming from the SHF cannot be excluded.

FACS analysis revealed that the first wave of *Fgf10* expression accounts for ~0.5% of the total lung at E18.5, whereas the second wave accounts for ~1.5% of the total E18.5 lung. This indicates that during embryonic lung development, not all *Fgf10*-expressing cells derive from *Fgf10*-positive mother cells; rather, the *Fgf10*-expressing domain expands by *de novo* induction of *Fgf10* expression (Fig. 8B). However, clonal expansion of *Fgf10*-positive cells needs to be further examined using confetti or rainbow Cre-reporter mice in order to assess the degree of heterogeneity of these cells and to determine whether they possess unipotent or multipotent capabilities. Flow cytometry analysis also revealed that a subpopulation of early and late lineage-labeled cells acquires *Pdgfra* expression at later developmental stages. Surprisingly, a subpopulation of late *Fgf10*-positive progenitors (second wave) also acquires *Epcam* expression. Epcam$^+$ RFP$^+$ cells were further analyzed following FACS and they showed lack of *Nkx2.1* and *E-Cad* expression, indicating that these cells do not represent a bona fide epithelial cell population. Yet they express significant levels of Pro-Spc, as shown by immunofluorescence (of lung sections and sorted cells) and RT-PCR, and appear to have lost *Fgf10* expression between P2 and P30. To date, there is no evidence for mesenchymal-to-epithelial transition events during lung development, and our previous work with the *Dermo1-Cre; R26R* line suggests that mesenchymal cells do not integrate into the lung epithelium (De Langhe et al., 2008; Tiozzo et al., 2012). Similarly, we show here that the *Fgf10*-expressing lineage is purely mesenchymal by nature and labeled cells were never detected in the lung epithelium. Whether these cells could ‘completely’ differentiate into bona fide epithelial cells under specific conditions (acute injury, for example) remains to be established.

Alveolar myofibroblasts and lipofibroblasts are two cell lineages that are highly abundant during postnatal alveolarization. These cell types play important roles in the formation of functional alveoli in newborns. In this study, the contribution of *Fgf10*-positive cells to these two lineages was addressed. When labeled during the alveolar

Development (2014) doi:10.1242/dev.099747

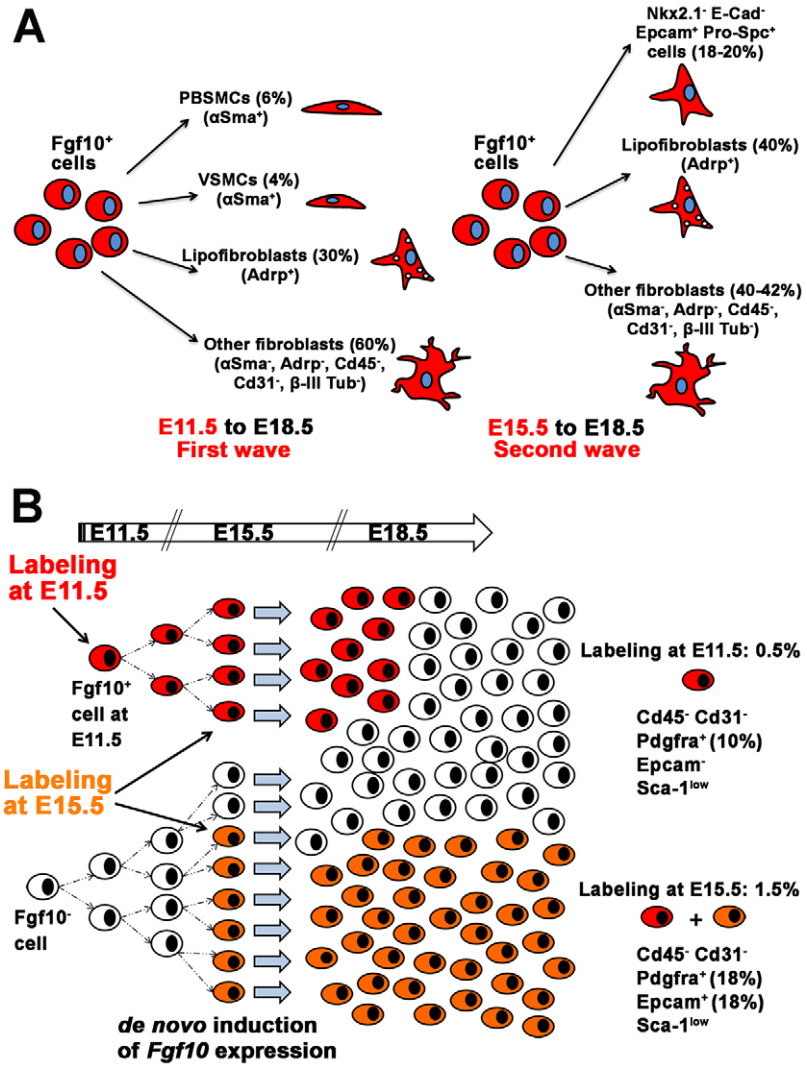

Fig. 8. The differentiation potential of *Fgf10*-positive cells varies throughout embryonic lung development. (A) Model showing the differentiation capacity of *Fgf10*-positive cells labeled at E11.5 or E15.5 and analyzed at E18.5. (B) Model showing that the *Fgf10*-expressing domain expands by *de novo* induction of *Fgf10* expression.

stage of lung development, most *Fgf10*-expressing cells gave rise to lipofibroblasts that are believed to represent a stem cell niche that signals to adjacent type 2 alveolar epithelial cells in a paracrine fashion (Barkauskas et al., 2013). Furthermore, a minor population of *Fgf10*-expressing cells gave rise to myofibroblasts residing in the parenchyma rather than in secondary septae. Alveolar myofibroblasts are believed to derive from *Pdgfra*-positive cells as *Pdgfa*-null newborns suffer from arrest in alveologenesis because of the absence of these cells (Boström et al., 1996; Lindahl et al., 1997). More recently, McGowan et al. have shown that *Pdgfra* expression directly correlated with *αSma* expression and inversely correlated with neutral lipid production (McGowan et al., 2008), indicating that *Pdgfra*-positive cells are progenitors for alveolar myofibroblasts rather than lipofibroblasts. Our FACS analysis shows that only ~10% of *Fgf10*-expressing cells co-express *Pdgfra* postnatally (data not shown), which could explain our observation that *Fgf10*-expressing cells preferentially give rise to lipofibroblasts rather than alveolar myofibroblasts ($Pdgfra^+$). Lipofibroblasts originate from multiple progenitor pools and the *Fgf10*-expressing pool contributes to a subset of lipofibroblasts in the lung (D.A.A., E.E.A. and S.B., unpublished). Although it has been suggested that lipofibroblasts serve as a source of alveolar myofibroblasts during alveologenesis (Perl and Gale, 2009), our data suggest that at least *Fgf10*-expressing lipofibroblasts do not undergo this transdifferentiation. However, as Fgfr2b ligands have shown to be required for the formation of alveolar myofibroblasts during homeostasis (Perl and Gale, 2009; Ramasamy et al., 2007) as well as regeneration after pneumonectomy (Chen et al., 2012), we speculate that paracrine signaling between *Fgf10*-positive cells and *Pdgfra*-positive progenitors is likely to be necessary for the formation of the alveolar myofibroblast lineage during alveologenesis.

Fgf10-positive cells were also examined during lung homeostasis in the adult mouse. Despite the low efficiency of the $Fgf10^{iCre}$ line in labeling *Fgf10*-expressing cells postnatally (El Agha et al., 2012), FACS analysis of disaggregated adult lungs revealed that these cells constitute ~0.1% of the whole lung. A subpopulation of *Fgf10*-expressing cells (~10.5% of total *Fgf10*-expressing cells) exhibits the molecular signature of resident MSCs ($Cd45^-$ $Cd31^-$ $Sca\text{-}1^+$) that were previously described by McQualter et al. (McQualter et al., 2009). In the latter study, the authors reported that the $Cd45^-$ $Cd31^-$ $Sca\text{-}1^+$ fraction of the adult lung represents a mesenchymal population of resident progenitor cells that are also crucial for the growth of epithelial progenitors *in vitro*. Our data support the findings of McQualter et al. and provide direct evidence that *Fgf10* expression identifies a subset of resident MSCs.

Finally, *Fgf10*-positive cells, labeled at E11.5, were retained after birth (P30), indicating that these cells have self-renewal

capabilities. Nevertheless, the majority of these cells stained for the neutral lipid dye, indicating their engagement into the lipofibroblast phenotype.

In summary, the reported genetic model of lineage tracing shows that *Fgf10*-expressing cells represent a population of mesenchymal progenitors in the lung *in vivo*. These cells give rise to airway and VSMCs as well as lipofibroblasts during embryonic development. Neonatally, these cells contribute to the formation of lipofibroblasts and during adult life, they represent a subset of resident MSCs that might play a crucial role in regeneration after lung injury. Our observation that some descendants of *Fgf10*-expressing cells express Pro-Spc shows how little is known about lineage hierarchy in the lung mesenchyme. More studies need to be performed in order to better characterize the various mesenchymal lineages in the lung, by combining lineage-tracing tools with responder lines allowing genetic manipulation of key signaling pathways (e.g. FGF, Wnt, Hedgehog), and eventually implementing the attained knowledge in novel therapeutic strategies for treating interstitial lung diseases.

MATERIALS AND METHODS

Mice and tamoxifen administration

Fgf10^{iCre} knock-in mice were generated as previously described (El Agha et al., 2012) and *tomato*^{flox} reporter mice (B6;129S6-*Gt(ROSA)26Sor*$^{tm9(CAG-tdTomato)Hze}$/J) were purchased from Jackson Lab (stock number 007905). *Fgf10-lacZ* hypomorph/reporter mice were described previously (Kelly et al., 2001; Mailleux et al., 2005; Ramasamy et al., 2007). Mice were housed in a specific pathogen-free environment and E0.5 was assigned to the day when a vaginal plug was detected. Harvesting organs and tissues from wild-type and transgenic mice was approved by Justus Liebig University Giessen (approval numbers 405_M and 437_M, respectively) and animal experiments were approved by the Regierungspraesidium Giessen (GI 20/10 Nr. 38/2011 and 117/2012) and the Animal Research Committee at Childrens Hospital Los Angeles (CHLA; Protocol number 31-11) in strict accordance with the recommendations in the Guide for the Care and Use of Laboratory Animals of the National Institute of Health. The approval identification for CHLA is AAALAC A3276-01.

Tamoxifen solution was prepared as previously described (El Agha et al., 2012) and pregnant females carrying *Fgf10*$^{iCre/+}$; *tomato*$^{flox/+}$ embryos received a single IP injection of 0.1 mg tamoxifen (Sigma, Schnelldorf, Germany) per gram of body weight. For continuous tamoxifen exposure, mice were fed tamoxifen-containing pellets (0.4 g of tamoxifen per kg of food) (Altromin, Lage, Germany).

Whole-mount fluorescence imaging and time-lapse microscopy

Lungs were harvested in PBS and examined using Leica M205 FA fluorescent stereoscope (Leica Microsystems, Wetzlar, Germany) equipped with Leica DFC360 FX camera. The endogenous tomato signal was detected using the RFP channel. For time-lapse microscopy, intact E12.5 lungs or E18.5 lung explants were harvested in Dulbecco's modified Eagle medium (DMEM) and cultured on Whatman Nuclepore membrane filters (GE Healthcare, Solingen, Germany) placed on 500 µl of DMEM with 10% fetal bovine serum (FBS) and 1% penicillin/streptomycin. Culture dishes with embryonic tissues were then transferred into the culture chamber (37°C; 5% CO_2) of Leica DMI6000 B live imaging microscope (Leica Microsystems) connected to Leica DFC365 FX camera where imaging was performed. RFP signal intensity was measured using ImageJ software (NIH).

Tissue processing and immunostaining

Freshly isolated lungs were washed in PBS and then fixed in 4% paraformaldehyde (PFA) in PBS according to standard procedures. Then, tissues were embedded in paraffin and sectioned at 5 µm thickness. Slides were deparaffinized, blocked with 3% bovine serum albumin (BSA) and 0.4% Triton X-100 [in Tris-buffered saline (TBS)] at room temperature (RT) for 1 hour and then incubated with primary antibodies against αSma (Sigma; 1:100), Adipose differentiation-related protein (Adrp) (Abcam; 1:50), Pro-Spc (Seven Hills; 1:1000), E-Cadherin (BD; 1:200), β-III Tubulin (R&D; 1:50), Cd45 or Cd31 (Biolegend; 1:100) at RT for 1 hour or at 4°C overnight. After incubation with primary antibodies, slides were washed three times in TBST (TBS buffer + 0.1% Tween 20) for 5 minutes, incubated with secondary antibodies at RT for 1 hour and then washed three times in TBST before being mounted with Prolong Gold Anti-fade Reagent with DAPI (4′,6-diamidino-2-phenylindole; Invitrogen). Fluorescent images were acquired using Leica DM5500 B fluorescence microscope connected to Leica DFC360 FX camera and the endogenous tomato signal was detected using the RFP channel. Colocalization data were further confirmed by *z* stacks of multiple optical sections using Leica TCS SP5 X confocal microscope.

FACS analysis and sorting

Lungs were isolated, washed with Hanks' balanced salt solution (HBSS) and kept on ice. Then, they were cut into fine pieces using a sharp blade before being digested with 0.5% Collagenase Type IV in HBSS (Life Technologies, Invitrogen) at 37°C for 45 minutes. Single-cell suspensions were obtained by passing lung homogenates through 18, 21 and 24G syringes before being passed through 70 and 40 µm cell strainers (BD Biosciences, Heidelberg, Germany). Viable cell count was determined using Trypan Blue stain. Cells were then resuspended in cold staining solution (0.1% sodium azide/5% FCS/0.05% Triton X-100 in 1× PBS) containing antibodies (Biolegend, Fell, Germany) against Cd45 (FITC-conjugated; 1:100), Cd31 (FITC-conjugated; 1:100), Epcam (APC-Cy7-conjugated; 1:50), Sca-1 (Pacific Blue-conjugated; 1:100), Pdgfra (APC-conjugated; 1:100) and Kit (PE-Cy7-conjugated; 1:50) for 30 minutes on ice in the dark and were then washed with 0.1% sodium azide in PBS. LipidTOX staining was performed according to the manufacturer's instructions (Invitrogen). FACS measurements and sorting were carried out using a FACSAria III cell sorter (BD Biosciences) and the endogenous tomato signal was detected using the PE channel. Gates were set according to unstained controls.

Figure assembly

Quantitative data were assembled using GraphPad Prism software (GraphPad Software) and presented as average values ± s.e.m. Figures were assembled using Adobe Photoshop CS5.

Acknowledgements

We would like to thank Matthew Jones for his help in genotyping the mice used for these experiments, Jana Roskovius for contributing to the immunofluorescence protocol, Kerstin Goth for efficiently managing mouse colonies at the Justus Liebig University Giessen and Salma Dilai for her help with processing the movies. We also acknowledge Oleg Pak for his help with confocal microscopy. Finally, we would like to thank Jonathan Branch, Clarence Wigfall and Soula Danopoulos for their technical support at CHLA.

Competing interests

The authors declare no competing financial interests.

Author contributions

S.B., P.M. and W.S. conceived the study; E.E.A. and S.B. designed the experiments; S.B., S.H. and D.A.A. contributed to materials; E.E.A., D.A.A., J.Q., B.M., G.C., A.M. and C.-M.C. performed the experiments; E.E.A., S.H. and S.B. analyzed the data; E.E.A. and S.B. wrote the manuscript.

Funding

This work was funded by a German Research Foundation (DFG) grant [BE 4443/4-1 to S.B.]; a Landes-Offensive zur Entwicklung Wissenschaftlich-ökonomischer Exzellenz (LOEWE) grant (to S.B.); a Universities of Giessen and Marburg Lung Center (UGMLC) grant (to S.B. and S.H.); and by National Institutes of Health (NIH) grants [HL086322 to S.B.; and HL107307 to S.B. and P.M.]. P.M. was also supported by the Hastings Foundation. Deposited in PMC for release after 12 months.

Supplementary material

Supplementary material available online at
http://dev.biologists.org/lookup/suppl/doi:10.1242/dev.099747/-/DC1

References

Barkauskas, C. E., Cronce, M. J., Rackley, C. R., Bowie, E. J., Keene, D. R., Stripp, B. R., Randell, S. H., Noble, P. W. and Hogan, B. L. M. (2013). Type 2 alveolar cells are stem cells in adult lung. *J. Clin. Invest.* **123**, 3025-3036.

Bellusci, S., Grindley, J., Emoto, H., Itoh, N. and Hogan, B. L. (1997). Fibroblast growth factor 10 (FGF10) and branching morphogenesis in the embryonic mouse lung. *Development* **124**, 4867-4878.

Boström, H., Willetts, K., Pekny, M., Levéen, P., Lindahl, P., Hedstrand, H., Pekna, M., Hellström, M., Gebre-Medhin, S., Schalling, M. et al. (1996). PDGF-A signaling is a critical event in lung alveolar myofibroblast development and alveogenesis. *Cell* **85**, 863-873.

Chen, L., Acciani, T., Le Cras, T., Lutzko, C. and Perl, A.-K. T. (2012). Dynamic regulation of platelet-derived growth factor receptor α expression in alveolar fibroblasts during realveolarization. *Am. J. Respir. Cell Mol. Biol.* **47**, 517-527.

Crapo, J. D., Barry, B. E., Gehr, P., Bachofen, M. and Weibel, E. R. (1982). Cell number and cell characteristics of the normal human lung. *Am. Rev. Respir. Dis.* **126**, 332-337.

De Langhe, S. P., Carraro, G., Tefft, D., Li, C., Xu, X., Chai, Y., Minoo, P., Hajihosseini, M. K., Drouin, J., Kaartinen, V., et al. (2008). Formation and differentiation of multiple mesenchymal lineages during lung development is regulated by beta-catenin signaling. *PLoS ONE* **3**, e1516.

Del Moral, P. M., Sala, F. G., Tefft, D., Shi, W., Keshet, E., Bellusci, S. and Warburton, D. (2006). VEGF-A signaling through Flk-1 is a critical facilitator of early embryonic lung epithelial to endothelial crosstalk and branching morphogenesis. *Dev. Biol.* **290**, 177-188.

Dixit, R., Ai, X. and Fine, A. (2013). Derivation of lung mesenchymal lineages from the fetal mesothelium requires hedgehog signaling for mesothelial cell entry. *Development* **140**, 4398-4406.

El Agha, E., Al Alam, D., Carraro, G., MacKenzie, B., Goth, K., De Langhe, S. P., Voswinckel, R., Hajihosseini, M. K., Rehan, V. K. and Bellusci, S. (2012). Characterization of a novel fibroblast growth factor 10 (Fgf10) knock-in mouse line to target mesenchymal progenitors during embryonic development. *PLoS ONE* **7**, e38452.

Giangreco, A., Reynolds, S. D. and Stripp, B. R. (2002). Terminal bronchioles harbor a unique airway stem cell population that localizes to the bronchoalveolar duct junction. *Am. J. Pathol.* **161**, 173-182.

Greif, D. M., Kumar, M., Lighthouse, J. K., Hum, J., An, A., Ding, L., Red-Horse, K., Espinoza, F. H., Olson, L., Offermanns, S. et al. (2012). Radial construction of an arterial wall. *Dev. Cell* **23**, 482-493.

Haan, N., Goodman, T., Najdi-Samiei, A., Stratford, C. M., Rice, R., El Agha, E., Bellusci, S. and Hajihosseini, M. K. (2013). Fgf10-expressing tanycytes add new neurons to the appetite/energy-balance regulating centers of the postnatal and adult hypothalamus. *J. Neurosci.* **33**, 6170-6180.

Hajihosseini, M. K., De Langhe, S., Lana-Elola, E., Morrison, H., Sparshott, N., Kelly, R., Sharpe, J., Rice, D. and Bellusci, S. (2008). Localization and fate of Fgf10-expressing cells in the adult mouse brain implicate Fgf10 in control of neurogenesis. *Mol. Cell. Neurosci.* **37**, 857-868.

Hong, K. U., Reynolds, S. D., Watkins, S., Fuchs, E. and Stripp, B. R. (2004). Basal cells are a multipotent progenitor capable of renewing the bronchial epithelium. *Am. J. Pathol.* **164**, 577-588.

Kappel, A., Rönicke, V., Damert, A., Flamme, I., Risau, W. and Breier, G. (1999). Identification of vascular endothelial growth factor (VEGF) receptor-2 (Flk-1) promoter/enhancer sequences sufficient for angioblast and endothelial cell-specific transcription in transgenic mice. *Blood* **93**, 4284-4292.

Kelly, R. G., Brown, N. A. and Buckingham, M. E. (2001). The arterial pole of the mouse heart forms from Fgf10-expressing cells in pharyngeal mesoderm. *Dev. Cell* **1**, 435-440.

Kim, C. F., Jackson, E. L., Woolfenden, A. E., Lawrence, S., Babar, I., Vogel, S., Crowley, D., Bronson, R. T. and Jacks, T. (2005). Identification of bronchioalveolar stem cells in normal lung and lung cancer. *Cell* **121**, 823-835.

Langsdorf, A., Radzikinas, K., Kroten, A., Jain, S. and Ai, X. (2011). Neural crest cell origin and signals for intrinsic neurogenesis in the mammalian respiratory tract. *Am. J. Respir. Cell Mol. Biol.* **44**, 293-301.

Lindahl, P., Karlsson, L., Hellström, M., Gebre-Medhin, S., Willetts, K., Heath, J. K. and Betsholtz, C. (1997). Alveogenesis failure in PDGF-A-deficient mice is coupled to lack of distal spreading of alveolar smooth muscle cell progenitors during lung development. *Development* **124**, 3943-3953.

Lü, J., Izvolsky, K. I., Qian, J. and Cardoso, W. V. (2005). Identification of FGF10 targets in the embryonic lung epithelium during bud morphogenesis. *J. Biol. Chem.* **280**, 4834-4841.

Mailleux, A. A., Kelly, R., Veltmaat, J. M., De Langhe, S. P., Zaffran, S., Thiery, J. P. and Bellusci, S. (2005). Fgf10 expression identifies parabronchial smooth muscle cell progenitors and is required for their entry into the smooth muscle cell lineage. *Development* **132**, 2157-2166.

McGowan, S. E., Grossmann, R. E., Kimani, P. W. and Holmes, A. J. (2008). Platelet-derived growth factor receptor-alpha-expressing cells localize to the alveolar entry ring and have characteristics of myofibroblasts during pulmonary alveolar septal formation. *Anat. Rec. (Hoboken)* **291**, 1649-1661.

McQualter, J. L. and Bertoncello, I. (2012). Concise review: Deconstructing the lung to reveal its regenerative potential. *Stem Cells* **30**, 811-816.

McQualter, J. L., Brouard, N., Williams, B., Baird, B. N., Sims-Lucas, S., Yuen, K., Nilsson, S. K., Simmons, P. J. and Bertoncello, I. (2009). Endogenous fibroblastic progenitor cells in the adult mouse lung are highly enriched in the sca-1 positive cell fraction. *Stem Cells* **27**, 623-633.

Nyeng, P., Norgaard, G. A., Kobberup, S. and Jensen, J. (2008). FGF10 maintains distal lung bud epithelium and excessive signaling leads to progenitor state arrest, distalization, and goblet cell metaplasia. *BMC Dev. Biol.* **8**, 2.

O'Hare, K. H. and Sheridan, M. N. (1970). Electron microscopic observations on the morphogenesis of the albino rat lung, with special reference to pulmonary epithelial cells. *Am. J. Anat.* **127**, 181-205.

Park, W. Y., Miranda, B., Lebeche, D., Hashimoto, G. and Cardoso, W. V. (1998). FGF-10 is a chemotactic factor for distal epithelial buds during lung development. *Dev. Biol.* **201**, 125-134.

Peng, T., Tian, Y., Boogerd, C. J., Lu, M. M., Kadzik, R. S., Stewart, K. M., Evans, S. M. and Morrisey, E. E. (2013). Coordination of heart and lung co-development by a multipotent cardiopulmonary progenitor. *Nature* **500**, 589-592.

Perl, A.-K. T. and Gale, E. (2009). FGF signaling is required for myofibroblast differentiation during alveolar regeneration. *Am. J. Physiol.* **297**, L299-L308.

Que, J., Wilm, B., Hasegawa, H., Wang, F., Bader, D. and Hogan, B. L. (2008). Mesothelium contributes to vascular smooth muscle and mesenchyme during lung development. *Proc. Natl. Acad. Sci. USA* **105**, 16626-16630.

Ramasamy, S. K., Mailleux, A. A., Gupte, V. V., Mata, F., Sala, F. G., Veltmaat, J. M., Del Moral, P. M., De Langhe, S., Parsa, S., Kelly, L. K. et al. (2007). Fgf10 dosage is critical for the amplification of epithelial cell progenitors and for the formation of multiple mesenchymal lineages during lung development. *Dev. Biol.* **307**, 237-247.

Rawlins, E. L., Clark, C. P., Xue, Y. and Hogan, B. L. M. (2009). The Id2+ distal tip lung epithelium contains individual multipotent embryonic progenitor cells. *Development* **136**, 3741-3745.

Rehan, V. K. and Torday, J. S. (2012). PPARγ signaling mediates the evolution, development, homeostasis, and repair of the lung. *PPAR Res.* **2012**, 289867.

Rock, J. R., Onaitis, M. W., Rawlins, E. L., Lu, Y., Clark, C. P., Xue, Y., Randell, S. H. and Hogan, B. L. (2009). Basal cells as stem cells of the mouse trachea and human airway epithelium. *Proc. Natl. Acad. Sci. USA* **106**, 12771-12775.

Rubin, L. P., Kovacs, C. S., De Paepe, M. E., Tsai, S.-W., Torday, J. S. and Kronenberg, H. M. (2004). Arrested pulmonary alveolar cytodifferentiation and defective surfactant synthesis in mice missing the gene for parathyroid hormone-related protein. *Dev. Dyn.* **230**, 278-289.

Sakaue, H., Konishi, M., Ogawa, W., Asaki, T., Mori, T., Yamasaki, M., Takata, M., Ueno, H., Kato, S., Kasuga, M. et al. (2002). Requirement of fibroblast growth factor 10 in development of white adipose tissue. *Genes Dev.* **16**, 908-912.

Shan, L., Subramaniam, M., Emanuel, R. L., Degan, S., Johnston, P., Tefft, D., Warburton, D. and Sunday, M. E. (2008). Centrifugal migration of mesenchymal cells in embryonic lung. *Dev. Dyn.* **237**, 750-757.

Srinivasan, R. S., Dillard, M. E., Lagutin, O. V., Lin, F.-J., Tsai, S., Tsai, M.-J., Samokhvalov, I. M. and Oliver, G. (2007). Lineage tracing demonstrates the venous origin of the mammalian lymphatic vasculature. *Genes Dev.* **21**, 2422-2432.

Stripp, B. R., Maxson, K., Mera, R. and Singh, G. (1995). Plasticity of airway cell proliferation and gene expression after acute naphthalene injury. *Am. J. Physiol.* **269**, L791-L799.

Tiozzo, C., Carraro, G., Al Alam, D., Baptista, S., Danopoulos, S., Li, A., Lavarreda-Pearce, M., Li, C., De Langhe, S., Chan, B. et al. (2012). Mesodermal Pten inactivation leads to alveolar capillary dysplasia- like phenotype. *J. Clin. Invest.* **122**, 3862-3872.

Torday, J. S. and Rehan, V. K. (2007). The evolutionary continuum from lung development to homeostasis and repair. *Am. J. Physiol.* **292**, L608-L611.

Vaccaro, C. and Brody, J. S. (1978). Ultrastructure of developing alveoli. I. The role of the interstitial fibroblast. *Anat. Rec.* **192**, 467-479.

Volckaert, T., Campbell, A., Dill, E., Li, C., Minoo, P. and De Langhe, S. (2013). Localized Fgf10 expression is not required for lung branching morphogenesis but prevents differentiation of epithelial progenitors. *Development* **140**, 3731-3742.

Yamada, M., Kurihara, H., Kinoshita, K. and Sakai, T. (2005). Temporal expression of alpha-smooth muscle actin and drebrin in septal interstitial cells during alveolar maturation. *J. Histochem. Cytochem.* **53**, 735-744.

Yamaguchi, T. P., Dumont, D. J., Conlon, R. A., Breitman, M. L. and Rossant, J. (1993). flk-1, an flt-related receptor tyrosine kinase is an early marker for endothelial cell precursors. *Development* **118**, 489-498.

Yamasaki, M., Emoto, H., Konishi, M., Mikami, T., Ohuchi, H., Nakao, K. and Itoh, N. (1999). FGF-10 is a growth factor for preadipocytes in white adipose tissue. *Biochem. Biophys. Res. Commun.* **258**, 109-112.